Clay bricks modified by implementing of N- and/or C-TiO_2: insight into self-cleaning properties toward fatty contaminant

Magdalena Janus[1] ✉, *Justyna Zatorska*[2], *Kamila Zając*[1], *Ewelina Kusiak-Nejman*[2], *Adam Czyżewski*[2], *Antoni Waldemar Morawski*[2]

[1]*Department of Sanitary Engineering, West Pomeranian University of Technology, Szczecin, al. Piastów 50, 70-310 Szczecin, Poland*
[2]*Institute of Chemical and Environmental Engineering, West Pomeranian University of Technology, Szczecin, ul. Pułaskiego 10, 70-322 Szczecin, Poland*
✉ *E-mail: mjanus@zut.edu.pl*

Published in Micro & Nano Letters; Received on 3rd May 2016; Revised on 16th September 2016; Accepted on 16th September 2016

Clay bricks containing different kinds of titanium dioxide (TiO_2) photocatalysts were obtained. The samples have shown high photocatalytic activity during thin layers of oleic acid deposited on their surface decomposition. The self-cleaning effectiveness of the bricks was evaluated on the basis of the water contact angle measurements, or more precisely, wettability rate (WR) changes on the greasy surface layers. It appeared that despite the high-temperature clay firing process (950°C), the presence of quartz and aluminosilicates in clay have caused the inhibition of anatase–rutile transformation. The highest photocatalytic efficiency, determined on the basis of the WR measurements, was observed for TiO_2/nitrogen (N) and TiO_2/N, carbon (C)-loaded bricks. It should be noted that in the case of the bricks loaded with the TiO_2/N,C photocatalyst, the carbon dopant present in the material was burnt out during the high-temperature kiln firing. The N content in latter samples show closely the same results (~0.03 and ~0.04 wt% of N for brick loaded with TiO_2/N and TiO_2/N,C, respectively). In the context of the photocatalytic activity of studied materials, the N presence was found to be one of the most important feature.

1. Introduction: Recently, there is a constantly growing demand to develop materials exhibiting high functionality, practical application, and enhanced energy conservation. The relatively new group of such materials, complementing the majority of above-mentioned requirements, are titanium dioxide (TiO_2)-loaded building materials revealing self-cleaning and antimicrobial properties. Moreover, it was confirmed that photoactive building materials (e.g. concrete, cement, and gypsum) are capable to efficiently decompose the gaseous or liquid deposits of potential pollutants or convert them to oxidised organic compounds, generally easily washed off from the surface with water or rain [1–3].

A common phenomenon the aesthetic of buildings and constructions is gradually lost over time. Building surfaces could be easily covered by greasy and sticky organic deposits. Greasy particles are adhered to building materials surface mainly by hydrocarbons and fatty acids [4]. The carboxylic groups of fatty acids enable the latter to adhere to the surface due to the formation of chemical bonds with the components present in building materials. It is also known that fatty residues may easily trap many dusts and other kinds of particles from the atmosphere [5]. Restoration of the aesthetic properties of soiled buildings requires the use of chemicals or expensive and energy consuming methods. An excellent solution to this problem could be the additive of photoactive TiO_2 to building materials and the obtainment of, e.g. self-cleaning bricks. It is worth pointing out that the current worldwide annual production of bricks is about 1391 billion units and the demand for bricks is expected to be continuously rising [6]. Conventional bricks are in the majority produced from clay with high-temperature kiln firing. The effort toward production of clay bricks with improved mechanical and thermal properties including incorporation of different particles into the clay mixture, creating voids during the firing process or reusing wastes from agricultural or industrial productions in the manufacture of clay brick are taken [7, 8].

It is worth pointing out that apart from photocatalytic activity of TiO_2, photo-induced hydrophilic properties of this semiconductor were merely observed [9, 10]. However, the hydrophilic properties of TiO_2 could be useful for the indirect photocatalytic degradation measurements of some fatty pollutants [1]. Namely, degradation of initial substrate leads to the formation of more hydrophilic compounds and finally gaseous products (i.e. CO_2, H_2O) as well as to the exposure of the hydrophilic TiO_2 surface. Hence, the photocatalytic decomposition of greasy deposits during irradiation can be ascertained by measuring the water contact angle changes.

Oleic acid (OA) (commonly used model fatty compound) is characterised by its suitable properties to simulate grease stains on various types of surfaces such as: double bond, low volatility, liquidity at room temperature, stability in the condensed phase, and ample occurrence. Rathouský *et al.* [1] showed that TiO_2 films with large surface area are photocatalytic efficient in the decomposition of thin layers of OA deposited by dip- or spray-coating on their surface. It was concluded that the oxidative degradation was induced by an attack of hydroxyl radical on the double bond of OA. Obata *et al.* [11] indicated that co-doping of TiO_2 [with tantalum and nitrogen (N)] enhanced the photocatalytic oxidation activity evaluated by the OA decomposition under visible light in comparison with N single doping.

In this Letter, the relation of bricks photoactivity, estimated during OA degradation under ultraviolet (UV) light, and physicochemical properties of the new composites loaded with TiO_2 modified with N and/or carbon (C) was investigated. Decomposition of OA contaminant was evaluated by applying the relatively simple method utilising the hydrophilic properties of the TiO_2 and intermediate products.

2. Experimental results

2.1. Materials: Raw clay (AS Keramik, Czech Republic) and anatase TiO_2 (supplied from Grupa Azoty Zakłady Chemiczne 'POLICE' S.A., Poland; denoted as starting TiO_2) were used as basic materials for the preparation of brick–TiO_2 composites. For reference, the additional brick material was prepared, containing commercial TiO_2 (P25, Evonik, Germany). Synthetic gaseous

© The Institution of Engineering and Technology 2016

doi: 10.1049/mnl.2016.0227

Table 1 Qualitative and quantitative composition of the prepared brick–TiO_2 materials

Material composition	Clay/photocatalyst weight ratio, wt%/wt%	Sample code
pure (TiO_2-free) brick	100/0	brick
brick + P25	90/10	brick–P25
brick + starting TiO_2	90/10	brick–stTiO_2
brick + TiO_2/N,C	90/10	brick–TiO_2/N,C
brick + TiO_2/C	90/10	Brick–TiO_2/C
brick + TiO_2/N	90/10	Brick–TiO_2/N

ammonia (purity 99.85%, Messer, Poland) and methanol (purity 99.80%, Avantor Performance Materials Poland S.A.) were used as N and C sources, respectively. Pure argon (purity 99.999%, Messer, Poland) was used as an inert gas. OA (purity 96%, Chempur, Poland), designated as OA, was employed as a model organic pollutant.

2.2. Preparation of N- and/or C-modified titania photocatalysts: Preparation method for modified TiO_2/N, TiO_2/C, or TiO_2/N,C photocatalysts obtained from crude TiO_2 was already described in detail in our earlier works [12]. The applied procedure briefly comprised of the following steps: (i) rinsing of crude TiO_2 with solution of ammonia water and then with distilled water, until pH value reached ca. 6.8, (ii) pre-drying of obtained TiO_2 slurry for 24 h at 90°C, and (iii) modification of the dried TiO_2 (denoted as starting TiO_2) with gaseous ammonia (N source) and/or methanol (C source) at 100°C for 1.5 h.

2.3. Preparation of brick–TiO_2 composites: At first, ground dried clay (115°C, 24 h) and the appropriate TiO_2-based photocatalyst were mechanically mixed at a weight ratio 90/10 (Table 1). The 10 wt% addition of photocatalysts into the clay matrix was chosen on the base of earlier studies, in which the addition was in the range from 1 to 20 wt%. In the case of modified clays, the optimal photocatalytic activity and mechanical properties were when the addition amounted 10 wt%. The obtained clay/titania mixtures were placed in porcelain mortar and thoroughly grinded. Subsequently, the acquired homogenous powders were blended with distilled water. The prepared slurries were poured into cubical moulds ($20 \times 20 \times 6$ mm^3) and kilned at 950°C for 5 h in muffle furnace.

2.4. Materials characterisation methods: The relative phase composition and crystalline structure of the tested photocatalysts, brick, and brick–TiO_2 composites were determined by X-ray diffraction (XRD) spectrometry (X'Pert PRO Philips diffractometer) using Cu Kα radiation ($\lambda = 0.154056$ nm). Raman spectra was performed by means of SuperGamut 532 OEM Raman spectrometer (BaySpec, Inc., USA), with the excitation wavelength of 532 nm. The differential thermal analyses (DTAs) were conducted using a Netzsch STA 449C precise thermobalance. The runs were carried out under synthetic air flow (30 cm^3/min) with heating rate of 10°C/min. N content in brick–TiO_2/N and brick–TiO_2/N,C samples was measured by ONH 836 elemental analyser (Leco Corporation, USA).

2.5. Determination of self-cleaning properties of the brick–TiO_2 composites: The self-cleaning properties of the prepared bricks were determined on the basis of the OA photodegradation measurements, conducted under six ultraviolet–visible (UV–vis) lamps (20 W each, Philips Cleo), with the radiation intensity of 110 W/m^2 for UV and 5 W/m^2 vis. Owing to the relatively low-vis

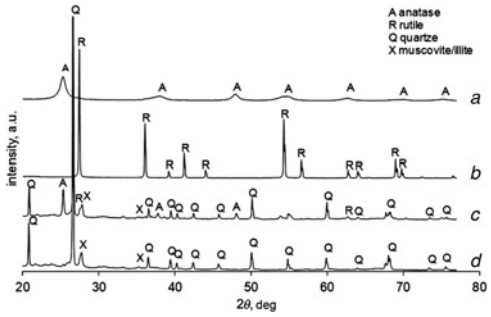


Fig. 1 *XRD patterns of the selected photocatalysts and bricks*
a TiO_2/N,C-100°C
b TiO_2/N,C-950°C
c Brick–TiO_2/N,C
d Pure brick

radiation intensity, the light source used in the experiments was considered as UV light, and henceforth denoted as UV irradiation. The employed procedure involved: (i) the uniform covering of the brick surface with the 50 µl of OA, (ii) the introduction of single water droplet on the greasy surface, and (iii) the determination of the WR of the sample measured after respective irradiation time (WR_{it}), defined by the following equation: $WR_{it} = (CA_i - CA_t)/t$, where CA_i is the initial contact angle, measured directly after deposition of the water droplet on stained sample, CA_t is the consecutive contact angle, measured in arbitrary selected time period ($t = 18$ s) after the deposition of the water droplet on stained sample. The contact angle measurements were conducted using the goniometer (Surface Energy Evaluation System, Advex Instruments). Water droplets were placed in three different positions for one sample and the average value was adopted as the contact angle. Standard deviations obtained on a single sample were of the order of a few degrees, which confirmed an acceptable reproducibility. The applied method was based on the assumption that the OA acts as a barrier blocking the contact between the hydrophilic brick surface and the deposited water droplet. Hence, the increase of the WR_{it} value (after respective UV irradiation time), may also indirectly indicate the decomposition rate of the OA, to the point of its complete removal.

The gradual decomposition of the OA on the surface of the brick–TiO_2 composite was also estimated by analysis the Fourier transform infrared spectroscopy (FTIR)/diffuse reflectance spectroscopy (DRS) spectra, obtained using FTIR 4200 spectrometer (Jasco, Japan) equipped with a diffuse reflectance accessory (Harrick, USA).

3. Results and discussion: It is well known that the increase of the treatment temperature, above ca. 600°C, alters the TiO_2 phase composition, from highly photoactive anatase phase to less active rutile form [13, 14]. However, we have obtained the N- and/or C-doped TiO_2-loaded photoactive bricks, revealing the presence

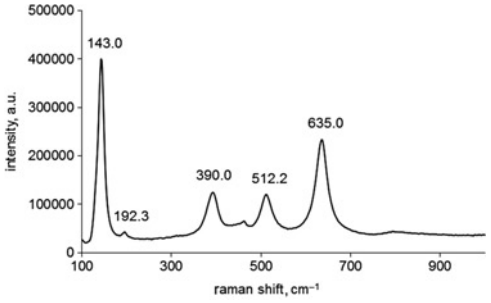


Fig. 2 *Raman spectrum of brick–TiO_2/N,C material*

© The Institution of Engineering and Technology 2016

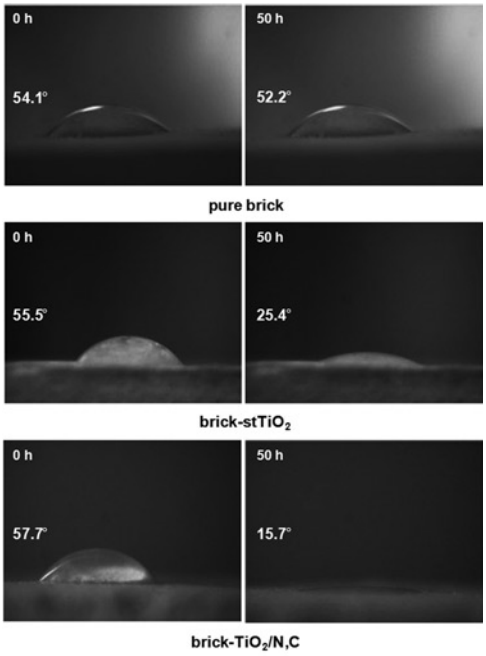


Fig. 3 *Photographs of water droplets placed on the surface of the OA-stained bricks, taken before (left) and after (right) 50 h of UV irradiation*

of anatase phase TiO_2, despite the fact that the respective bricks were prepared at 950°C. This fact was well shown in the XRD pattern of the exemplary brick–TiO_2/N,C sample (Fig. 1).

Similar phase composition (date not included) was also observed in the remaining brick–TiO_2 composites, separately modified with C or N elements. The XRD data were generally consisted with the results of the Raman analyses. As shown in Fig. 2, the Raman spectrum of exemplary brick–TiO_2/N,C sample, confirms the presence of, characteristic for anatase phase TiO_2 bands, vis at 143.0, 390.0, 512.2, and 635.0 cm^{-1} [15]. The observed inhibition of the anatase to rutile TiO_2 phase transformation in the brick–TiO_2 composite might be connected with the presence of the additional species in the clay material. Namely, the XRD data of the obtained composites (Fig. 1) reveal the presence of diffraction peaks originating from quartz (SiO_2) and additional aluminosilicate minerals, indentified as illite and muscovite. According to the literatures [16–18], both silica and alumina species can suppress the anatase–rutile phase transformation, even at very high treatment temperatures, ranging from 900 to 1200°C. Several research groups [19–21] generally agreed that SiO_2 and aluminium oxide species act as a barrier, capable of stabilising the anatase phase TiO_2, and as a result inhibiting its further transformation to less photoactive rutile form. In view of this finding, the prepared brick–TiO_2 composites might exhibit superior photocatalytic activity, leading to the efficient decomposition of the applied fatty contaminant.

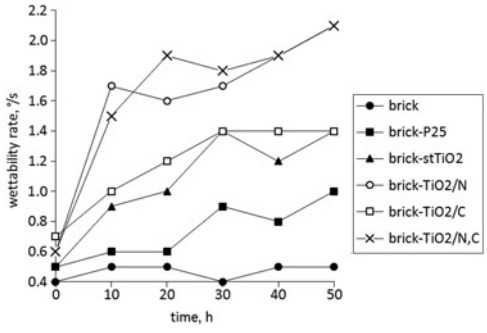


Fig. 4 *Photocatalytic performance under UV light irradiation of the prepared bricks in photodegradation of OA, expressed in the form of WR*

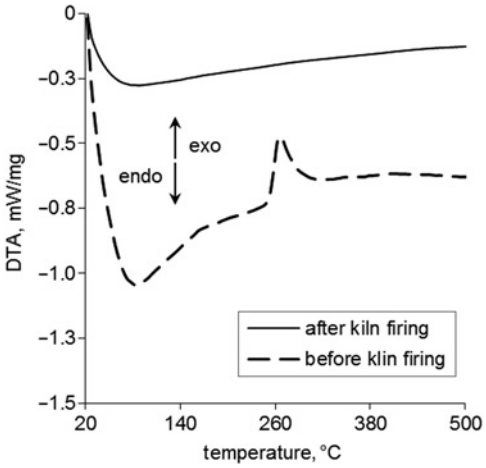


Fig. 5 *DTA curves of the brick–TiO_2/C samples, before and after kiln firing*

Fig. 3 illustrates the changes of water contact angles for the pure brick and representative brick–TiO_2 composites recorded before and after 50 h of UV irradiation. As it was explained in Section 2, the photocatalytic performance of the prepared brick–TiO_2 materials can be indirectly determined by measuring the changes of the initial and consecutive water droplet contact angle, expressed in the form of the WR (Fig. 4).

One should note that in contrast to the pure brick sample, the WR_{it} values of all the brick–TiO_2 composites progressively increased with the UV irradiation time. The observed difference was related with gradual degradation of OA on the surface of the composites. In comparison with the referential brick–P25 material, the obtained brick–TiO_2 composites, containing N- and/or C-modified TiO_2, exhibited significantly higher WR_{it} values. It ought to be noted that among this group of materials, the N- and N,C-doped brick–TiO_2 composites (brick–TiO_2/N and brick–TiO_2/N,C, respectively) exhibited closely similar WR_{it} values. The remaining brick–TiO_2/C material revealed surprisingly low WR_{it} values, comparable with those observed for the referential brick–stTiO_2 composite, containing unmodified photocatalyst. The described close similarity between the latter composites maybe explained by the results of the DTAs, conducted for the brick–TiO_2/C samples: one already kilned at 950°C and another not yet subjected to the kiln firing process (Fig. 5). The DTA curves of the respective samples commonly show endothermic peak, centred at ca. 85°C, related to the evaporation of adsorbed and interlayer water. In case of the DTA curve of the brick–TiO_2/C material before kiln firing, an additional exothermic peak was observed, at ca. 270°C, attributed to the burning of the C element of the C-modified TiO_2 photocatalysts present in the brick–TiO_2/C composite. Similar DTA data (not included) were also obtained for the remaining C- and N-doped brick–TiO_2 composite. In view of the obtained DTA results, it is believed that similar C burning step also occurred during the brick kiln firing process conducted in muffle furnace. The above given observations suggest that the presence of N dopant in the brick–TiO_2/N (~0.03 wt%) and brick–TiO_2/N,C (~0.04 wt%) materials was found to be the mean feature, determining the enhancement of the photoactivity of the brick–TiO_2 composites [22, 23].

The role of non-metal dopant in TiO_2 lattice was already explained in our earlier work [24]. It was also postulated in the literatures [25, 26] that the modification of TiO_2 with non-metals causes the occurrence of defects in TiO_2 lattice. The lattice impurities may suppress the recombination of photo-induced charge carriers.

The photodegradation of the OA covering the surface of the brick–TiO_2/N,C composite was also confirmed by the results of the FTIR/DRS analysis (Fig. 6).

The OA characteristic peaks, assigned to C–H stretching vibrations of alkyl groups, were found at 2853 and 2920 cm^{-1}. On the

© The Institution of Engineering and Technology 2016

doi: 10.1049/mnl.2016.0227

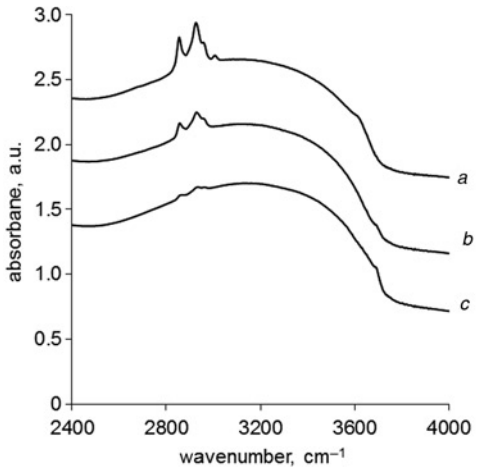


Fig. 6 *FTIR/DRS spectra of OA-stained brick–TiO_2/N,C samples measured*
a Before and after 50 h
b Before and after 500 h
c Of UV irradiation

basis of the comparison of the FTIR spectra of brick–TiO_2/N,C samples before and after 50 h of UV irradiation, it was clearly shown that the OA peaks intensity of the latter sample significantly decreased. The extension of the irradiation time to 500 h resulted in further reduction of the OA bands intensity. However, even after such a long irradiation time, the total removal of OA molecules was not reached due to the formation of a large number of intermediates. These co-products are considered as competitive toward the OA molecules in the photodegradation process [27, 28].

4. Conclusion: The new group of clay bricks containing N- and/or C-modified TiO_2 photocatalysts were successfully obtained. On the basis of conducted studies, the following conclusions were reached:

- SiO_2 and aluminosilicates present in clay matrix stabilise the anatase phase TiO_2, inhibiting its further transformation to less photoactive rutile form (kiln firing conducted at 950°C);

- the N modification of TiO_2 photocatalysts causes the enhancement of the TiO_2-loaded bricks photocatalytic activity, determined on the basis of OA degradation under UV light irradiation; and

- the lower photoactivity of TiO_2/C-loaded bricks is related to the fact that C in TiO_2/C photocatalyst burnt out during the kiln firing process.

5. Acknowledgment: This work was supported by The National Centre for Research and Development, LIDER III programme (Lider/14/30/L-3/11/NBCIR/2012).

6 References

[1] Rathouský J., Kalousek V., Kolář M., *ET AL.*: 'A study into the self-cleaning surface properties – the photocatalytic decomposition of oleic acid', *Catal. Today*, 2011, **161**, pp. 202–208
[2] Chen J., Kou S.C., Poon C.S.: 'Photocatalytic cement-based materials: comparison of nitrogen oxides and toluene removal potentials and evaluation of self-cleaning performance', *Build. Environ.*, 2011, **46**, pp. 1827–1833
[3] Wang F., Yang L., Sun G., *ET AL.*: 'The hierarchical porous structure of substrate enhanced photocatalytic activity of TiO_2/cementitious materials', *Constr. Build. Mater.*, 2014, **64**, pp. 488–495
[4] Chen J., Poon C.S.: 'Photocatalytic construction and building materials: from fundamentals to applications', *Build. Environ.*, 2009, **44**, pp. 1899–1906
[5] Folli A., Pade C., Bæk Hansen T., *ET AL.*: 'TiO_2 photocatalysis in cementitious systems: insights into self-cleaning and depollution chemistry', *Cement Concr. Res.*, 2012, **42**, pp. 539–548
[6] Zhang L.: 'Production of bricks from waste materials – a review', *Constr. Build. Mater.*, 2013, **47**, pp. 643–655
[7] Bories C., Borredon M.E., Vedrenne E., *ET AL.*: 'Development of eco-friendly porous fired clay bricks using pore-forming agents: A review', *J. Environ. Manage.*, 2014, **143**, pp. 186–196
[8] Muńoz P., Morales M.P., Mendívil M.A., *ET AL.*: 'Using of waste pomace from winery industry to improve thermal insulation of fired clay bricks. Eco-friendly way of building construction', *Constr. Build. Mater.*, 2014, **71**, pp. 181–187
[9] Yu J.C., Yu J., Ho W., *ET AL.*: 'Light-induced super-hydrophilicity and photocatalytic activity of mesoporous TiO_2 thin films', *J. Photochem. Photobiol. A, Chem.*, 2002, **148**, pp. 331–339
[10] Fujishima A., Zhang X., Tryk D.A.: 'TiO_2 photocatalysis and related surface phenomena', *Surf. Sci. Rep.*, 2008, **63**, pp. 515–582
[11] Obata K., Irie H., Hashimoto K.: 'Enhanced photocatalytic activities of Ta, N co-doped TiO_2 thin films under visible light', *Chem. Phys.*, 2007, **339**, pp. 124–132
[12] Janus M., Bubacz K., Zatorska J., *ET AL.*: 'Self-cleaning properties of cement plates loaded with N,C-modified TiO_2 photocatalysts', *Appl. Surf. Sci.*, 2015, **330**, pp. 200–206
[13] Yuangpho N., Le S.T.T., Treerujiraphapong T., *ET AL.*: 'Enhanced photocatalytic performance of TiO_2 particles via effect of anatase–rutile ratio', *Physica E*, 2015, **67**, pp. 18–22
[14] Ovenstone J., Yanagisawa K.: 'Effect of hydrothermal treatment of amorphous titania on the phase change from anatase to rutile during calcinations', *Chem. Mater.*, 1999, **11**, pp. 2770–2774
[15] Kusiak-Nejman E., Wanag A., Kowalczyk L., *ET AL.*: 'Modification of titanium dioxide with graphitic carbon from anthracene thermal decomposition as a promising method for visible-active photocatalysts preparation', *J. Adv. Oxid. Technol.*, 2016, **19**, pp. 227–235
[16] Anderson C., Bard A.J.: 'Improved photocatalytic activity and characterization of mixed TiO_2/SiO_2 and TiO_2/Al_2O_3 materials', *J. Phys. Chem. B*, 1997, **101**, pp. 2611–2616
[17] Fu X., Clark L.A., Yang Q., *ET AL.*: 'Enhanced photocatalytic performance of titania-based binary metal oxides: TiO_2/SiO_2 and TiO_2/ZrO_2', *Environ. Sci. Technol.*, 1996, **30**, pp. 647–653
[18] Anderson C., Bard A.J.: 'An improved photocatalyst of TiO_2/SiO_2 prepared by a sol–gel synthesis', *J. Phys. Chem.*, 1995, **99**, pp. 9882–9885
[19] Nilchi A., Janitabar-Darzi S., Mahjoub A.R., *ET AL.*: 'New TiO_2/SiO_2 nanocomposites. Phase transformations and photocatalytic studies', *Colloid. Surf. A*, 2010, **361**, pp. 25–30
[20] Tobaldi D.M., Tucci A., Skapin A.S., *ET AL.*: 'Effects of SiO_2 addition on TiO_2 crystal structure and photocatalytic activity', *J. Eur. Ceram. Soc.*, 2010, **30**, pp. 2481–2490
[21] Zhao J., Wang Y., Lou X., *ET AL.*: 'Effects of adding Al_2O_3 on the crystal structure of TiO_2 and the performance of Pd-based catalysts supported on the composite for the total oxidation of ethanol', *Inorg. Chim. Acta*, 2013, **405**, pp. 395–399
[22] Kuo Y.L., Su T.L., Kung F.C., *ET AL.*: 'A study of parameter setting and characterization of visible-light driven nitrogen-modified commercial TiO_2 photocatalysts', *J. Hazard. Mater.*, 2011, **190**, pp. 938–944
[23] Giannakas A.E., Seristatidou E., Deligiannakis Y., *ET AL.*: 'Photocatalytic activity of N-doped and N-F co-doped TiO_2 and reduction of chromium (VI) in aqueous solution: an EPR study', *Appl. Catal. B, Environ.*, 2013, **132-133**, pp. 460–468
[24] Janus M., Bubacz K., Zatorska J., *ET AL.*: 'Preliminary studies of photocatalytic activity of gypsum plasters containing TiO_2 co-modified with nitrogen and carbon', *Pol. J. Chem. Technol.*, 2015, **17**, pp. 96–102
[25] Wang X., Lim T.T.: 'Solvothermal synthesis of C-N codoped TiO_2 and photocatalytic evaluation for bisphenol A degradation using a visible-light irradiated LED photoreactor', *Appl. Catal. B, Environ.*, 2010, **100**, pp. 355–364
[26] Linsebigler A.L., Lu G., Yates J.T.: 'Photocatalysis on TiO_2 surfaces: principles, mechanisms and selected results', *Chem. Rev.*, 1995, **95**, pp. 735–758
[27] Eng Y.Y., Sharma V.K., Ray A.K.: 'Photocatalytic degradation of nonionic surfactant, Brij 35 in aqueous TiO_2 suspensions', *Chemosphere*, 2010, **79**, pp. 205–209
[28] Gumy D., Giraldo S.A., Rengifo J., *ET AL.*: 'Effect of suspended TiO_2 physicochemical characteristics on benzene derivatives photocatalytic degradation', *Appl. Catal. B, Environ.*, 2008, **78**, pp. 19–29

© The Institution of Engineering and Technology 2016